

## Electronic structure of Ni<sup>+</sup> in I<sub>B</sub>-III-VI<sub>2</sub> chalcopyrite semiconductors

U. Kaufmann

*Institut für Angewandte Festkörperphysik der Fraunhofer-Gesellschaft, 7800 Freiburg, Federal Republic of Germany*

(Received 7 October 1974)

Electron-spin-resonance (ESR) and optical-absorption spectra of Ni<sup>+</sup> (3d<sup>9</sup>) impurities have been observed in the ternary chalcopyrite compounds CuAlS<sub>2</sub>, CuGaS<sub>2</sub>, and AgGaS<sub>2</sub>. Identification of the axial ESR centers as being due to Ni has been confirmed by the observation of hyperfine structure in crystals enriched with <sup>61</sup>Ni. Large axial-field splittings due to the tetragonal crystal-field component in the chalcopyrite structure are inferred from the ESR and optical data. All experimental results can be consistently interpreted within the framework of static crystal-field theory. A complete set of crystal-field parameters is obtained for Ni<sup>+</sup> in each of the three hosts. No evidence for a Jahn-Teller effect is found.

### I. INTRODUCTION

During the last few years much work has been done on ternary I<sub>B</sub>-III-VI<sub>2</sub> and II<sub>B</sub>-IV-V<sub>2</sub> semiconductors.<sup>1,2</sup> These compounds usually crystallize in the tetragonal chalcopyrite (ch) structure, I $\bar{4}2d$ , which derives directly from the cubic zinc-blende lattice. Interest in these materials has arisen mainly because of their nonlinear optical properties.

Defect studies on I<sub>B</sub>-III-IV<sub>2</sub> compounds have so far concentrated on iron impurities<sup>3-8</sup> and on the 3d<sup>7</sup> ions Co<sup>2+</sup> and Ni<sup>3+</sup>.<sup>9</sup> This paper deals with electron spin resonance (ESR) and optical absorption of Ni<sup>+</sup> (3d<sup>9</sup>) in CuAlS<sub>2</sub>, CuGaS<sub>2</sub>, and AgGaS<sub>2</sub>. Previous work on 3d<sup>9</sup> ions on trigonally and approximately tetragonally distorted tetrahedral sites has been summarized by Bates and Chandler<sup>10</sup> and by Schulz.<sup>11</sup> The present study gives the first complete analysis of a d<sup>9</sup> ion on a purely tetragonally distorted tetrahedral site. Ground-state *g* factors and hyperfine constants as well as line positions and intensity ratios in the optical spectra are interpreted in terms of static-crystal-field theory including effects of covalency. The correlation between ESR and optical data yields parameter sets which describe consistently all experimental observations for Ni<sup>+</sup> in the three different hosts.

Jahn-Teller effects are known to play an important role in interpreting the properties of many d<sup>9</sup> ions on tetrahedral or slightly distorted tetrahedral sites.<sup>10,12</sup> However, for the examples presented here such effects will be shown to be of little importance. This greatly simplifies the theoretical analysis. The setup for the optical-absorption measurements has been described elsewhere.<sup>13</sup> ESR spectra were recorded at 20 K using Varian X- and Q-band spectrometers. Crystals have been grown by chemical transport with Ni added to the starting materials. The nominal

Ni concentration varied between 100 and 1000 ppm. Most optical data were obtained using natural {112} facets. In the case of AgGaS<sub>2</sub>, however, it was possible to cut a {110} facet sufficiently large for optical investigations. The thickness of the specimens was about 0.1 cm.

### II. THEORY

#### A. Energy-level scheme

In an external magnetic field the crystal-field Hamiltonian for a Ni<sup>+</sup> ion on a S<sub>4</sub> distorted tetrahedral cation site of the ch structure reads

$$\mathcal{H} = V_{\text{cub}} + V_{\text{ttr}} + \lambda_0 k \vec{L} \cdot \vec{S} + \mu_B (k \vec{L} + g_e \vec{S}) \cdot \vec{H}. \quad (1)$$

Here  $V_{\text{cub}}$  and  $V_{\text{ttr}}$  are the tetrahedral and tetragonal parts of the crystalline potential, see, e.g., Vallin *et al.*<sup>14</sup>  $\lambda_0$  is the free-ion spin-orbit coupling constant of Ni<sup>+</sup> and  $g_e$  is the free-electron *g* factor. In a first approximation covalency effects have been incorporated into this Hamiltonian by substituting  $k\vec{L}$  for  $\vec{L}$  where  $k$  is a covalency reduction factor. Two different values  $k$  and  $k'$  have to be used for matrix elements of  $\vec{L}$  within the  $t_2$  orbitals and for matrix elements between the  $t_2$  and  $e$  orbitals. The corresponding effective spin-orbit coupling constants are then given by  $\lambda = k\lambda_0$  and  $\lambda' = k'\lambda_0$ . In an axial crystal both  $k$  and  $k'$  are anisotropic. Strictly speaking one thus has four different orbital reduction factors. To keep the number of unknown parameters as small as possible we neglect any anisotropy in  $k$  and  $k'$ . As a further approximation we set  $k' = \sqrt{k}$ . It is shown in the Appendix that this approximation is reasonable for Ni<sup>+</sup> in a tetrahedral environment.

Assuming  $V_{\text{cub}} > V_{\text{ttr}} > \lambda \vec{L} \cdot \vec{S}$ , the free-ion ground state <sup>2</sup>D of Ni<sup>+</sup> is split by the crystalline field as shown in Fig. 1. By definition positive values of the tetragonal-crystal-field parameters  $\delta$  and  $\mu$  stabilize the <sup>2</sup>B(*T*<sub>2</sub>) and <sup>2</sup>B(*E*) state, respectively.<sup>15,16</sup>

This corresponds to the case actually observed for Ni<sup>+</sup> in the ch crystals investigated here. Inclusion of spin-orbit coupling gives rise to five Kramers doublets labeled  $K_i$  ( $i=1, 5$ ) in Fig. 1. Their energies correct to the order  $\lambda^2/10Dq$  are

$$E(K_5) = 6Dq + \frac{1}{2}\mu + \frac{\frac{3}{2}\lambda'^2}{10Dq - \frac{1}{3}\delta + \frac{1}{2}\mu - \frac{1}{2}|\lambda|}, \quad (2a)$$

$$E(K_4) = 6Dq - \frac{1}{2}\mu + \frac{\lambda'^2}{10Dq - \frac{1}{2}\mu - E_+} \times \left( \frac{1}{\sqrt{2}} \cos\omega - \sin\omega \right)^2 + \frac{\lambda'^2}{10Dq - \frac{1}{2}\mu - E_-} \left( \cos\omega + \frac{1}{\sqrt{2}} \sin\omega \right)^2, \quad (2b)$$

$$E(K_3) = -4Dq + \frac{1}{3}\delta + \frac{1}{2}|\lambda| - \frac{\frac{3}{2}\lambda'^2}{10Dq - \frac{1}{3}\delta + \frac{1}{2}\mu - \frac{1}{2}|\lambda|}, \quad (2c)$$

$$E(K_2) = -4Dq + E_+ - \frac{\lambda'^2}{10Dq - \frac{1}{2}\mu - E_+} \times \left( \frac{1}{\sqrt{2}} \cos\omega - \sin\omega \right)^2, \quad (2d)$$

$$E(K_1) = -4Dq + E_- - \frac{\lambda'^2}{10Dq - \frac{1}{2}\mu - E_-} \times \left( \cos\omega + \frac{1}{\sqrt{2}} \sin\omega \right)^2, \quad (2e)$$

where

$$E_{\pm} = \frac{1}{2}\delta \left( \frac{1}{2}\eta - \frac{1}{3} \pm S \right), \\ \sin^2\omega = \frac{1}{2} \left[ 1 - \left( 1 + \frac{1}{2}\eta \right) / S \right], \\ \cos^2\omega = \frac{1}{2} \left[ 1 + \left( 1 + \frac{1}{2}\eta \right) / S \right], \\ \sin 2\omega = \sqrt{2} \eta / S, \\ S = \left[ \left( 1 + \frac{1}{2}\eta \right)^2 + 2\eta^2 \right]^{1/2}, \text{ and } \eta = \lambda / \delta.$$

### B. Relative intensities

Selection rules for transitions between the orbital and between the spin-orbit states are indicated by arrows in Fig. 1. In order to calculate intensity ratios we make the following simplifying assumptions: (i) The radial functions of  ${}^2E(T_2)$  and  ${}^2B(T_2)$  are assumed to be identical as well as those of  ${}^2A(E)$  and  ${}^2B(E)$ . (ii) Mixing of  $K_5$  with  $K_3$  and of  $K_4$  with  $K_2$  and  $K_1$  via spin-orbit interaction is neglected. With these approximations the perpendicular intensity of the transitions  $K_1 \rightarrow K_5$  and  $K_1 \rightarrow K_4$  is solely due to the mixing of  $K_1$  with  $K_2$  via  $\lambda \vec{L} \cdot \vec{S}$ . This mixing is expected to be the dominant mechanism in transferring perpendicular intensity into the above-mentioned transitions. One obtains

$$I_{\parallel}(K_1 \rightarrow K_5) / I_{\perp}(K_1 \rightarrow K_5) = 4 \cot^2\omega, \quad (3a)$$

$$I_{\perp}(K_1 \rightarrow K_4) / I_{\text{tot}}(K_1 \rightarrow K_5) = 3(E_{14}/E_{15})(4 \cot^2\omega + 1)^{-1}. \quad (3b)$$

$E_{15}$ , for instance, means  $|E(K_1) - E(K_5)|$ . These intensity ratios can conveniently be compared with experiment.

### C. Spin Hamiltonian

If  $|\lambda| < |\delta|$  either  $K_1$  or  $K_2$  is the ground state of a  $d^9$  ion ( $\lambda < 0$ ) depending on the sign of  $\delta$ . As mentioned earlier,  $\delta > 0$  for the systems investigated in this work, hence  $K_1$  lies lowest. Neglecting quadrupole effects the spin Hamiltonian of  $K_1$  reads

$$\mathcal{H} = g_{\parallel} \mu_B H_z S_z + g_{\perp} \mu_B (H_x S_x + H_y S_y) + A_{\parallel} I_z S_z + A_{\perp} (I_x S_x + I_y S_y).$$

The hyperfine term applies only to the Ni<sup>61</sup> isotope ( $I = \frac{3}{2}$ , natural abundance 1.25%), all other Ni isotopes having  $I = 0$ . The  $z$  axis is taken along the  $c$  axis.

The  $g$  factors and hyperfine constants correct to the order  $\lambda/\Delta$  have been calculated including covalency but neglecting effects due to the mixing with excited electron configurations. Crystal-field theory predicts

$$g_{\parallel} = g_e \cos 2\omega - 2k \sin^2\omega - (4k'\lambda'/\Delta) \times (2 \cos^2\omega + \frac{1}{2}\sqrt{2} \sin 2\omega), \quad (4a)$$

$$g_{\perp} = g_e \cos^2\omega - \sqrt{2} k \sin 2\omega + (\sqrt{2} k'\lambda'/\Delta) \times (\sin 2\omega + \sqrt{2} \sin^2\omega), \quad (4b)$$

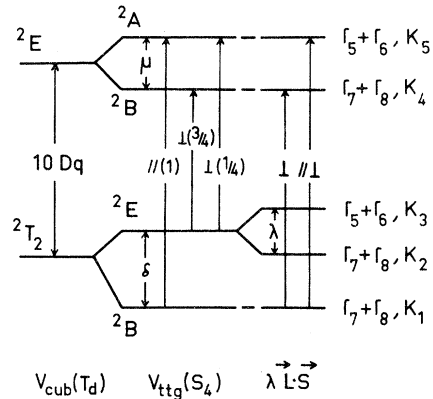


FIG. 1. Energy-level scheme of a  $d^9$  ion on a tetragonally distorted tetrahedral site. Electric dipole selection rules for  $\vec{E} \parallel \vec{c}$  and  $\vec{E} \perp \vec{c}$  and relative transition probabilities are indicated.

$$A_{\parallel} = P \left[ -\frac{4}{7} + 2\left(\frac{1}{7} - k\right) \sin^2 \omega - \kappa \cos 2\omega - \frac{3}{7} \sqrt{2} \sin 2\omega - (4\lambda'/\Delta) \left( 2k' \cos^2 \omega + \frac{3}{14} \sin^2 \omega + \frac{1}{28} \sqrt{2} (3 + 14k') \sin 2\omega \right) \right], \quad (5a)$$

$$A_{\perp} = P \left[ \left( \frac{2}{7} - \kappa \right) \cos^2 \omega - \sqrt{2} \left( k - \frac{3}{14} \right) \sin 2\omega - (\sqrt{2} \lambda'/\Delta) \left( \frac{3}{14} - k' \right) (\sin 2\omega + \sqrt{2} \sin^2 \omega) \right]. \quad (5b)$$

Here  $\Delta = 10Dq - \frac{1}{2}\mu + |E_{-}|$  and  $P = 2g_N \mu_N \mu_B \langle r^{-3} \rangle_{3d}$ .  $\kappa$  measures the core polarization. Using  $\langle r^{-3} \rangle_{3d} = 6.42$  a.u. for  $\text{Ni}^{2+}$ ,<sup>17</sup> one gets  $P(\text{Ni}^{61}) = 102 \times 10^{-4} \text{ cm}^{-1}$ .  $\kappa$  should be near 0.3 for a  $3d^9$  ion.<sup>17</sup>

### III. EXPERIMENTAL RESULTS

#### A. Optical spectra

Figures 2–4 show the absorption spectra of  $\text{CuAlS}_2:\text{Ni}$ ,  $\text{CuGaS}_2:\text{Ni}$ , and  $\text{AgGaS}_2:\text{Ni}$  in the 2–3  $\mu\text{m}$  region at  $\approx 4.2$  K. In each case there is a high-energy band predominantly polarized  $\vec{E} \parallel \vec{c}$  and a much weaker band at lower energy polarized  $\vec{E} \perp \vec{c}$ ; they are labeled  $\alpha$  and  $\beta$ , respectively. In  $\text{CuGaS}_2:\text{Ni}$  the band at higher energy is superimposed on a very broad structureless absorption extending from about 2.1  $\mu\text{m}$  up to 0.65  $\mu\text{m}$ .<sup>9</sup> For  $\text{CuAlS}_2:\text{Ni}$  and  $\text{AgGaS}_2:\text{Ni}$  no crystal-field transitions higher in energy than those of Figs. 2 and 4 could be observed. However, in  $\text{AgGaS}_2:\text{Ni}$  a structureless absorption starts near 1.0  $\mu\text{m}$  and beyond 0.6  $\mu\text{m}$  the crystals are no longer transparent. The group of weak lines marked with an asterisk in Figs. 2 and 3 possibly does not arise from that center which is responsible for the bands  $\alpha$  and  $\beta$ .

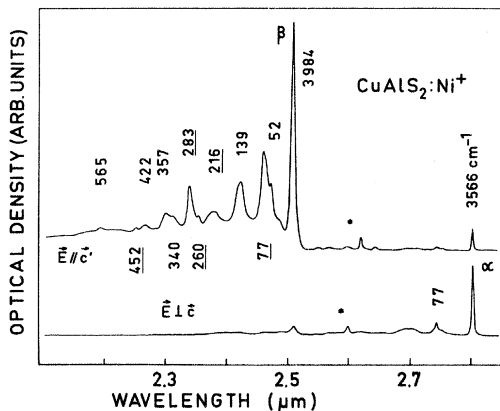


FIG. 2. Absorption spectrum of  $\text{CuAlS}_2:\text{Ni}^{2+}$  at 4.2 K. The numbers attached to the phonon sidebands measure the energy separation from line  $\beta$  in wave numbers. Note that  $c'$  makes an angle of  $\approx 35^\circ$  with the  $c$  axis since the spectrum has been obtained from a  $\{112\}$  face.

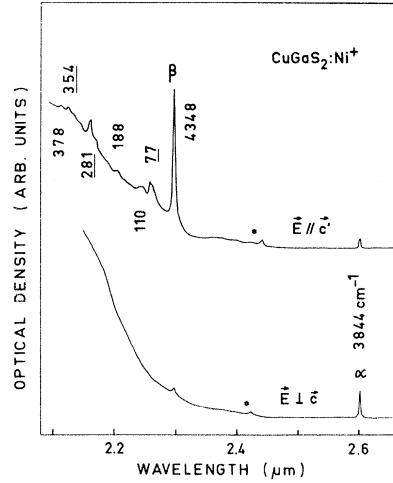


FIG. 3. Absorption spectrum of  $\text{CuGaS}_2:\text{Ni}^{2+}$  at 4.2 K as obtained from a  $\{112\}$  face.

#### B. ESR

As grown crystals of  $\text{CuAlS}_2:\text{Ni}$ ,  $\text{CuGaS}_2:\text{Ni}$ , and  $\text{AgGaS}_2:\text{Ni}$  usually exhibit two different axial ESR centers. The first center has been ascribed previously to  $\text{Ni}^{3+}$ .<sup>9</sup> The  $g$  factors of the second center are listed in Table I. We assign it to  $\text{Ni}^{2+}$ .

Annealing in  $\text{Cu}_2\text{S}$  strongly enhances the  $\text{Ni}^{2+}$  signal and quenches the  $\text{Ni}^{3+}$  signal. Samples enriched with  $\approx 80$ -at. %  $\text{Ni}^{61}$  ( $I = \frac{3}{2}$ ) did not exhibit a well-resolved four-line hyperfine pattern in the case of  $\text{AgGaS}_2:\text{Ni}$ . However, as Fig. 5 shows there is no doubt that this line arises from a Ni center. The hyperfine splitting in  $\text{CuAlS}_2:\text{Ni}$  and  $\text{CuGaS}_2:\text{Ni}$  was well resolved for  $\vec{H} \perp \vec{c}$ , see Fig. 6, but not for  $\vec{H} \parallel \vec{c}$ . The hyperfine parameters  $A_{\parallel}$  and  $A_{\perp}$  are included in Table I. In  $\text{AgGaS}_2:\text{Ni}$  ligand hyperfine structure is resolved for  $H \parallel c$ , see Fig. 7. Whereas the  $\text{Ni}^{2+}$  signal in  $\text{CuGaS}_2$  and

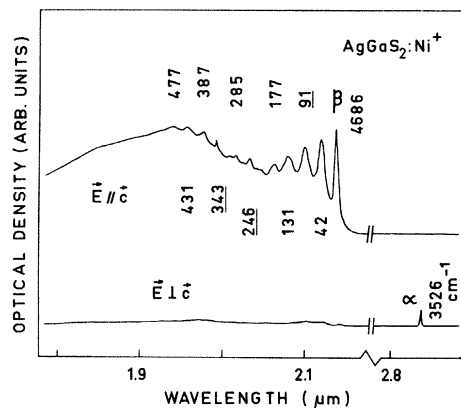


FIG. 4. Absorption spectrum of  $\text{AgGaS}_2:\text{Ni}^{2+}$  at 4.2 K.

TABLE I. ESR parameters of  $\text{Ni}^+$  in  $\text{I}_B\text{-III-VI}_2$  compounds (20 K).

Host	$g_{\parallel}$		$g_{\perp}$		$ A_{\parallel} $ ( $10^{-4} \text{ cm}^{-1}$ )		$ A_{\perp} $ ( $10^{-4} \text{ cm}^{-1}$ )		$k$	$\eta$
	Expt.	Eq. (4a)	Expt.	Eq. (4b)	Expt.	Eq. (5a)	Expt.	Eq. (5b)		
$\text{CuAlS}_2$	2.051	2.037	2.330	2.467	$\leq 13$	10.2	61	52.0	0.68	-0.45
$\text{CuGaS}_2$	1.915	1.921	2.324	2.464	$< 15$	4.3	62	53.0	0.68	-0.47
$\text{AgGaS}_2$	2.645	2.681	2.220	2.304	$< 17$	16.8	$< 36$	28.5	0.66	-0.22

$\text{CuAlS}_2$  could only be observed below  $\approx 40$  K it is easily detected at 80 K in  $\text{AgGaS}_2$ . In crystals where the  $\text{Ni}^+$  ESR signal had been quenched by sulphur anneal also the sharp optical absorption lines in Figs. 2-4 had vanished.

#### IV. INTERPRETATION OF EXPERIMENTAL RESULTS

##### A. Optical spectra

Our ESR studies show that the Ni centers described in III B have axial symmetry. Inspection of the ch lattice shows that there are no interstitial sites having axial symmetry. We therefore conclude that Ni either occupies the monovalent group- $\text{I}_B$  and/or the trivalent group-III sites. Thus the most probable charge states are  $\text{Ni}^+$  and  $\text{Ni}^{3+}$ . However, the possibility of  $\text{Ni}^{2+}$  on either site cannot be ruled out *a priori*.<sup>9</sup>

If the bands shown in Figs. 2-4 are assigned to  $\text{Ni}^+$  one has to ascertain that they do not arise from  $\text{Ni}^{3+}$  and/or  $\text{Ni}^{2+}$  since the isoelectronic, divalent impurities  $\text{Co}^{2+}$ ,  $\text{Ni}^{2+}$ , and  $\text{Cu}^{2+}$  in ZnS all exhibit absorption bands between 1.5 and 3  $\mu\text{m}$ .<sup>12,18,19</sup> For  $\text{CuAlS}_2$  and  $\text{AgGaS}_2$   $\text{Ni}^{2+}$  and  $\text{Ni}^{3+}$  are readily ruled out by the fact that crystal-field bands higher in energy than those of Figs. 2 and 4 have not been observed.

In  $\text{CuGaS}_2$  crystal-field transitions of  $\text{Ni}^{3+}$  and/or  $\text{Ni}^{2+}$  occurring at wavelengths smaller than 2.0

$\mu\text{m}$  might be obscured by the broad absorption between 2.1 and 0.65  $\mu\text{m}$ . As already mentioned the sharp lines in Fig. 3 together with the ESR signal described in Sec. III B had vanished after sulphur anneal whereas the  $\text{Ni}^{3+}$  ESR signal was quite prominent. Hence the sharp lines in Fig. 3 are unlikely due to  $\text{Ni}^{3+}$ . Though we cannot definitely rule out the possibility of  $\text{Ni}^{2+}$ , the similarity to the case of  $\text{AgGaS}_2$  and  $\text{CuAlS}_2$  strongly favors  $\text{Ni}^+$ .

If it is accepted that the sharp absorption lines in Figs. 2-4 arise from  $\text{Ni}^+$  it is immediately clear from the polarization selection rules, see Fig. 1, that the axial field stabilizes the  ${}^2B(T_2)$  state. The lines  $\alpha$  and  $\beta$  in Figs. 2-4 are therefore assigned to the zero-phonon transitions  $K_1 \rightarrow K_4$  and  $K_1 \rightarrow K_5$ , respectively. The residual intensity of the former line for  $\vec{E} \parallel \vec{c}'$  in the case of  $\text{CuAlS}_2:\text{Ni}$  and  $\text{CuGaS}_2:\text{Ni}$  is due to the fact that the  $c'$  axis makes an angle of  $\approx 35^\circ$  with the  $c$  axis. The remaining structure is attributed to phonon sidebands of lines  $\beta$ . A complete analysis of these sidebands in terms of host lattice phonons at critical points is not possible at present since available data<sup>20,21</sup> comprise only zone center modes. While the underlined sideband frequencies can be identi-

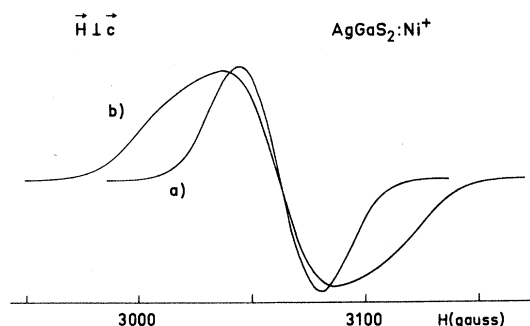


FIG. 5. ESR signal of  $\text{Ni}^+$  in  $\text{AgGaS}_2$  under  $\vec{H} \perp \vec{c}$ , 20 K, 9.5 GHz; (a) natural Ni isotope ratio; (b) enriched with  $\approx 80\text{-at.}\% \text{Ni}^{61}$ .

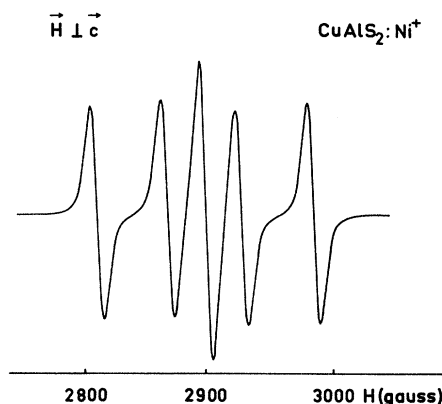


FIG. 6. ESR signal of  $\text{Ni}^+$  (enriched with  $\approx 80\text{-at.}\% \text{Ni}^{61}$ ) in  $\text{CuAlS}_2$  under  $\vec{H} \perp \vec{c}$ ; 20 K, 9.5 GHz. The four-line hyperfine pattern arises from  $\text{Ni}^{61}$ , the central line is due to other Ni isotopes having  $I=0$ .

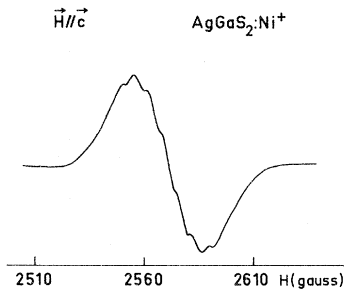


FIG. 7. ESR signal of  $\text{Ni}^+$  (natural isotope ratio) in  $\text{AgGaS}_2$  under  $\vec{H} \parallel \vec{c}$ ; 20 K, 9.5 GHz. Note the occurrence of ligand hyperfine structure from the next-nearest-neighbor shell.

fied with zone center modes the residual ones probably correspond to modes at the boundary of the Brillouin zone. However, local mode effects cannot be excluded. Using Eqs. (3a) and (3b) intensity ratios have been calculated with the  $\eta$  values obtained from the ESR data. They agree qualitatively with experiment (see Table II). Better agreement should not be expected since the experimental intensity ratios are only rough estimates which may be in error by as much as 40%. The crystal field parameters  $Dq$  and  $\mu$  are now easily obtained using Eqs. (2a)–(2e) and the  $k$  and  $\eta$  values derived from the ESR data. These parameters are listed in Table II.

### B. ESR

In all crystals of  $\text{CuGaS}_2:\text{Ni}$ ,  $\text{CuAlS}_2:\text{Ni}$ , and  $\text{AgGaS}_2:\text{Ni}$  exhibiting the sharp absorptions of Figs. 2–4 the ESR signal described in Sec. III B was most prominent. It is therefore assigned to  $\text{Ni}^+$ . The four line hyperfine pattern observed from crystals enriched with  $\approx 80$ -at. %  $\text{Ni}^{61}$  demonstrates that this signal indeed arises from a Ni center. The ligand hyperfine structure observed for  $\text{AgGaS}_2:\text{Ni}$  must be due to the next nearest neighbor shell containing Ag and Ga since the nearest neighbor shell is formed by sulphur. This indicates considerable delocalization of the hole and covalency effects are expected to be important.

TABLE II. Crystal-field parameters of  $\text{Ni}^+$  in  $I_B$ -III- $\text{VI}_2$  compounds at 4.2 K (energies in  $\text{cm}^{-1}$ ).

Host	$Dq$	$\delta$	$\mu$	$\frac{I_{\parallel}(K_1 \rightarrow K_5)}{I_{\perp}(K_1 \rightarrow K_5)}$		$\frac{I_{\perp}(K_1 \rightarrow K_4)}{I_{\text{tot}}(K_1 \rightarrow K_5)}$	
				Expt.	Eq. (3a)	Expt.	Eq. (3b)
$\text{CuAlS}_2$	287	915	411	40	23	0.06	0.11
$\text{CuGaS}_2$	325	875	501	26	21	0.07	0.12
$\text{AgGaS}_2$	263	1815	1177	230	134	0.007	0.017

Though the  $g$  factors of the  $\text{Ni}^+$  center in the three  $I_B$ -III- $\text{VI}_2$  compounds are rather different it is possible to fit them using formulas (4a) and (4b). Note that there are only two free fitting parameters,  $k$  and  $\eta$ , since  $\Delta$  is known from the absorption spectra and  $\lambda_0 = -605 \text{ cm}^{-1}$  for the free  $\text{Ni}^+$  ion.<sup>22,23</sup> Table I shows that a good fit is obtained with  $k$  values near 0.65.

A check on the consistency of the parameter set  $\Delta$ ,  $k$ , and  $\eta$  can be obtained from the observed hyperfine splittings of  $\text{Ni}^{61}$ . If one uses  $P = 102 \times 10^{-4} \text{ cm}^{-1}$  and  $\kappa = 0.25$ , see Sec. IIC, together with the  $k$  and  $\eta$  values obtained from the  $g$ -factor fit one can predict  $A_{\parallel}$  and  $A_{\perp}$  from Eqs. (5a) and (5b). In view of the fact that all parameters entering these equations have been fixed, the agreement between calculated and observed values is quite good (see Table I).

### V. DISCUSSION AND CONCLUSION

It has been shown that the EPR and optical spectra of  $\text{Ni}^+$  in I-III- $\text{VI}_2$  compounds can be consistently interpreted in terms of static crystal-field theory including covalency. From the optical spectra one directly obtains the crystal-field parameters  $Dq$  and  $\mu$  while the parameters  $k$  and  $\eta$  can be extracted from the ground-state  $g$  factors. With  $\lambda = k\lambda_0$  and  $\lambda' = \sqrt{k}\lambda_0$  one then deduces the parameter set  $Dq, \mu, \delta, \lambda, \lambda'$  which fixes the  $d^9$  energy level scheme completely. This set has then successfully been used to predict intensity ratios in the optical spectra and the hyperfine constants of the  $\text{Ni}^+$  ground state in three different hosts. The good agreement between theory and experiment suggests that the most important approximations made in this work, namely, neglect of mixing with excited electronic configurations, of vibronic interactions and of anisotropy in  $k$  cannot be severe. They may, of course, be responsible for the small differences between calculated and experimental spin-Hamiltonian parameters.

Recent estimates of Chatterjee<sup>24</sup> and of Bates and Chandler<sup>10b</sup> for the  $4p$  admixture in tetrahedrally coordinated  $\text{Cu}^{2+}$  amount to about 4%. For  $\text{Ni}^+$  this figure should be nearly the same since  $10Dq$  divided by the energy separation between the free-ion configurations  $3d^9$  and  $3d^84p$  is almost equal for tetrahedrally coordinated  $\text{Cu}^{2+}$  and  $\text{Ni}^+$ .<sup>25</sup> Thus as long as terms of the order  $(\lambda/10Dq)^2$  are neglected it is of no use to include  $4p$  mixing in the expressions for the spin-Hamiltonian parameters since both approximations introduce errors of the same order of magnitude.

A linear vibronic interaction with asymmetric vibrational modes (Jahn-Teller effect) cannot occur in the ground state  ${}^2B(T_2)$  since it has no

orbital degeneracy. A Jahn-Teller effect may however be present in the first excited state  ${}^2E(T_2)$ . The fact that the tetragonal splitting of the cubic  ${}^2T_2$  state is quite large ( $\sim 1000 \text{ cm}^{-1}$ ) suggests that the coupling with  $T_2$  modes cannot be strong since such a coupling would tend to quench the tetragonal splitting.<sup>26</sup> On the other hand a weak  $T_2$ -mode coupling would hardly affect the  ${}^2B(T_2)$  state because of its large separation from  ${}^2E(T_2)$ . In the case of  $E$ -mode coupling there is no mixing at all between vibronic levels of  ${}^2B(T_2)$  and  ${}^2E(T_2)$  via the Jahn-Teller interaction. Therefore an  $E$ -mode Jahn-Teller effect within  ${}^2E(T_2)$  could affect the ground state only indirectly via spin-orbit coupling. This is probably the reason why static crystal-field theory works so well in the present case.

A final point worth mentioning is covalency. It was found that the orbital reduction factor  $k$  is close to 0.65 for Ni<sup>+</sup> in the three ternary sulfides investigated. This value appears reasonable in view of the fact that experimental and theoretical estimates yield essentially the same  $k$  value for  $3d^9$  centers in II-VI compounds.<sup>27</sup> In addition, the observation of ligand hyperfine structure due to the next nearest neighbor shell in the case of AgGaS<sub>2</sub>:Ni<sup>+</sup> confirms that a considerable portion of the Ni<sup>+</sup> hole density is centered on the ligands.

#### ACKNOWLEDGMENTS

I am greatly indebted to Dr. A. R uber and Professor J. Schneider for suggesting this work and for numerous helpful discussions. I am particularly grateful to Dr. P. Koidl for very useful comments on the manuscript. Thanks are also due to F. Friedrich and R. Moritz for growing the crystals.

#### APPENDIX: RELATION BETWEEN $k$ AND $k'$

In tetrahedral symmetry the central-ion  $t_2$  orbitals form  $\sigma$  bonds with the ligands while the  $e$  orbitals form  $\pi$  bonds only. If the effect of  $\pi$  bonding is neglected, which should be a reasonable approximation for tetrahedral coordination, a simple relation between  $k$  and  $k'$  can be derived provided that covalent bonding is not too large. The hybrid orbitals may be written as a linear combination of central-ion  $d$  orbitals and  $\sigma$  ligand orbitals

$$\begin{aligned} |t_2\tau\rangle &= N(d_\tau - \rho\sigma_\tau) \quad (\tau = \xi, \eta, \zeta), \\ |e\tau'\rangle &= d_{\tau'} \quad (\tau' = \theta, \epsilon). \end{aligned} \quad (\text{A1})$$

$N$  is a normalization constant and  $\rho$  the admixture coefficient.

Defining the reduction factors in the usual way,

$$\begin{aligned} k &= \frac{\langle t_2\xi | L_z | t_2\eta \rangle}{\langle d_\xi | L_z | d_\eta \rangle}, \\ k' &= \frac{\langle e\epsilon | L_z | t_2\xi \rangle}{\langle d_\epsilon | L_z | d_\zeta \rangle}, \end{aligned}$$

and inserting the appropriate hybrid orbitals (A1) one obtains

$$k = N^2(1 - 2\rho S), \quad k' = N(1 - \rho S).$$

In writing the same overlap integral  $S$  in the expressions for  $k$  and  $k'$  we have assumed that the radial parts of all  $d$  orbitals are the same. If  $2\rho S \ll 1$  it follows that  $k' \approx N(1 - 2\rho S)^{1/2}$ . Hence

$$k' \approx \sqrt{k}. \quad (\text{A2})$$

In the case of ZnSe:Ni<sup>+</sup> Watts<sup>17</sup> finds  $S \approx 0.13$  and  $\rho \approx 0.74$  giving  $2\rho S \approx 0.19$ . One can therefore expect that relation (A2) is also a reasonable approximation for Ni<sup>+</sup> in the ternary compounds investigated here.

<sup>1</sup>J. L. Shay and J. H. Wernick, *Ternary Chalcopyrite Semiconductors—Growth, Electronic Properties, and Applications* (Pergamon, New York, 1974).

<sup>2</sup>U. Kaufmann and J. Schneider, in *Festk rperprobleme XIV—Advances in Solid State Physics* (Vieweg-Pergamon, Braunschweig, 1974).

<sup>3</sup>J. Schneider, A. R uber, and G. Brandt, *J. Phys. Chem. Solids* **34**, 443 (1973).

<sup>4</sup>T. Teranishi, K. Sato, and K. Kondo, *J. Phys. Soc. Jpn.* **36**, 1618 (1974).

<sup>5</sup>T. Kambara, *J. Phys. Soc. Jpn.* **36**, 1625 (1974).

<sup>6</sup>G. Brandt, A. R uber, and J. Schneider, *Solid State Commun.* **12**, 481 (1973).

<sup>7</sup>J. v. Bardeleben, B. Meyer, A. Goltz n , and C. Schwab (unpublished).

<sup>8</sup>K. Sato and T. Teranishi, *J. Phys. Soc. Jpn.* **37**, 415 (1974).

<sup>9</sup>U. Kaufmann, A. R uber, and J. Schneider, *Solid*

*State Commun.* **15**, 1881 (1974).

<sup>10</sup>C. A. Bates and P. E. Chandler, *J. Phys. C* **4**, 2713 (1971); **6**, 1975 (1973).

<sup>11</sup>M. Schulz, *Solid State Commun.* **11**, 1161 (1972).

<sup>12</sup>H. Maier and U. Scherz, *Phys. Status Solidi B* **62**, 153 (1974).

<sup>13</sup>K. Leutwein, *Appl. Opt.* **10**, 46 (1971).

<sup>14</sup>J. T. Vallin, G. A. Slack, S. Roberts, and A. E. Hughes, *Phys. Rev. B* **2**, 4313 (1970).

<sup>15</sup>We use Mullikan's notation and that of Ref. 16 to denote the transformation properties of orbital states and of spin-orbit states, respectively.

<sup>16</sup>G. F. Koster, J. O. Dimmock, R. G. Wheeler, and H. Statz, *Properties of the Thirty-two Point Groups* (M.I.T., Cambridge, Mass., 1963).

<sup>17</sup>R. K. Watts, *Phys. Rev.* **188**, 568 (1969).

<sup>18</sup>U. Kaufmann, P. Koidl, and O. F. Schirmer, *J. Phys. C* **6**, 310 (1973).

- <sup>19</sup>P. Koidl, O. F. Schirmer, and U. Kaufmann, *Phys. Rev. B* 8, 4926 (1973).
- <sup>20</sup>W. H. Koschel, V. Hohler, A. Räuber, and J. Baars, *Solid State Commun.* 13, 1011 (1973).
- <sup>21</sup>J. P. van der Ziel, A. E. Meixner, H. M. Kasper, and J. A. Ditzenberger, *Phys. Rev. B* 9, 4286 (1974).
- <sup>22</sup>B. N. Figgis, *Introduction to Ligand Fields* (Wiley, New York, 1966).
- <sup>23</sup>A. Abragam and B. Bleaney, *Electron Paramagnetic Resonance of Transition Ions* (Oxford U. P., London, 1970).
- <sup>24</sup>R. Chatterjee, *Can. J. Phys.* 47, 1 (1969).
- <sup>25</sup>C. E. Moore, *Natl. Bur. Stds. Circular No. 467* (U.S. GPO, Washington, D.C., 1971).
- <sup>26</sup>F. S. Ham, *Phys. Rev.* 138, A1727 (1965).
- <sup>27</sup>A. F. J. Cox and W. E. Hagston, *J. Phys. C* 3, 1954 (1970).